Electronic Supplementary Material (ESI) for Energy & Environmental Science.

Electronic Supplementary Information

A Spontaneous Hydrogen Fuel Purifier under Truly Ambient Weather Conditions

Ritwik Mondal,[1#] Ravikumar Thimmappa,[1#] Bhojkumar Nayak,[1] Anweshi Dewan,[1] Mruthyunjayachari Chattanahalli Devendrachari,[1] Qingsong Chen,[2] Zhenhai Wen,[2*] Musthafa Ottakam Thotiyl[1*]

[1]Department of Chemistry and Centre for Energy Science, Indian Institute of Science Education and Research, Pune, Dr. Homi Bhabha Road, Pune, 411008, India

[2]CAS Key Laboratory of Design and Assembly of Functional Nanostructures, and Fujian Provincial Key Laboratory of Materials and Techniques toward Hydrogen Energy, Fujian Institute of Research on the Structure of Matter, Chinese Academy of Sciences, Fuzhou, Fujian, 350002, China.

*Correspondence: musthafa@iiserpune.ac.in, wen@fjirsm.ac.cn

# These authors contributed equally.

Calculation S1

Water formation Reaction from H^+ and OH^- dual ions

$H^+ + OH^- \leftrightarrow H_2O$

Enthalpy changes for the reaction.

$\Delta H^0 = H^0 (H_2O) – H^0 (H^+) – H^0 (OH^-)$

$= – 285.8 – 0 – (– 230)$

$=$ **$– 55.8$ kJ/mol**

Entropy changes for the reaction

$\Delta S^0 = S^0 (H_2O) –S^0 (H^+) – S^0 (OH^-)$

$= 69.91 – 0 – (– 10.75)$

$=$ **0.08066 kJ/K mol**

Gibbs free energy of the reaction

$\Delta G^0 = \Delta H^0 – T\Delta S^0$

$= – 55.8 – (298 * 0.08066)$

$=$ **$– 79.875$ kJ/mol**

$\Delta G^0 = – nFE^0$

$E^0 = – \Delta G^0 /nF$

$E^0 = – (– 79875)/1*96484$

$E^0 =$ **0.82 V**

0.82 V of electromotive force can be harvested from the water formation energy.

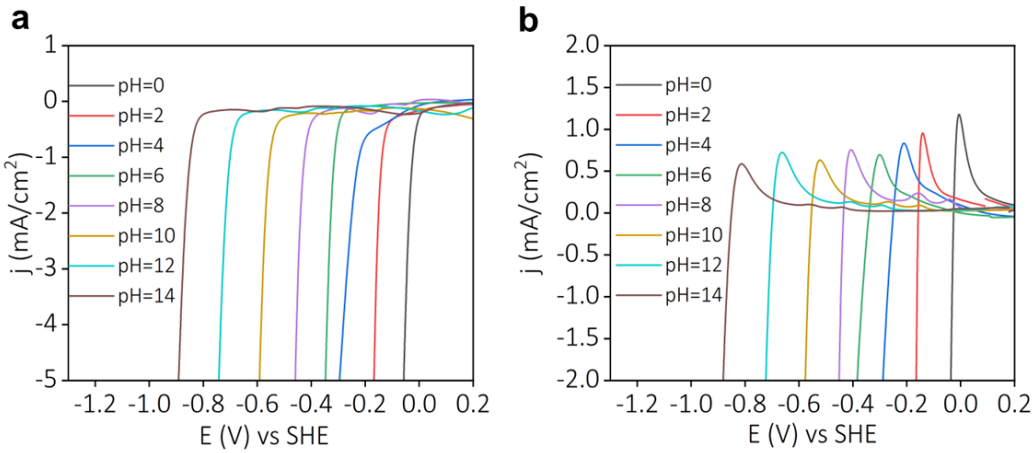

Fig. S1. (a**)** Hydrogen evolution reactions and (b) Hydrogen oxidation reactions in different pH solutions at a scan rate of 10 mV/s.

The half-cell reactions of direct interconversion of water formation energy

Anodic Half Cell Reaction

$2H_2O + 2e^- \leftrightarrow H_2 + 2OH^-$ $E^o_{SHE} = -0.82$ V **(equation S1)**

Cathodic Half Cell Reaction

$2H^+ + 2e^- \leftrightarrow H_2$ $E^o_{SHE} = 0$ V **(equation S2)**

Overall Cell Reaction

$2H^+ + 2OH^- \leftrightarrow 2H_2O$ $E^o_{Cell} = 0.82$ V **(equation S3)**

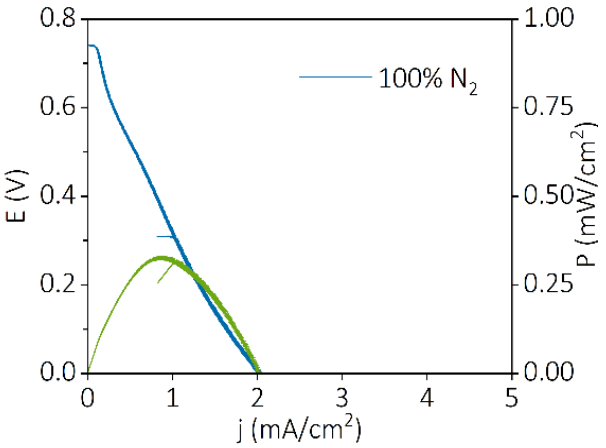

Fig. S2. Polarisation curve for hydrogen purifying device without H_2 fuel feed at the anodic half-cell.

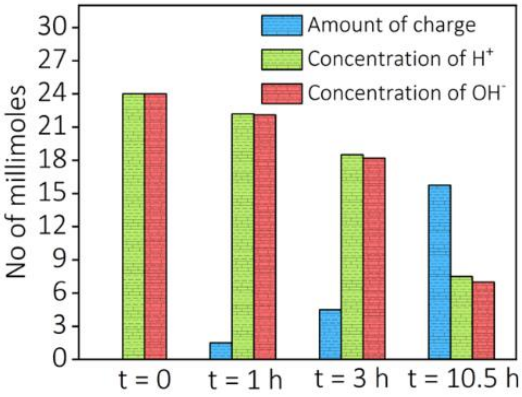

Fig. S3. Correlation between the charge passed and the remaining amount of H^+/OH^- dual ion concentration in the half cells during the long-term discharge. (Corresponding to Fig. 1d).

Calculation S2

The total cell reaction for the purifier is:

$H^+ (aq) + OH^- (aq) \rightarrow H_2O (l)$ …….. **equation S3**

The free energy change for that reaction can be written as follows:

$\Delta G = \Delta G^o + RT \ln \left({}^{product}/_{reactant}\right)$

$\Delta G_{Neutralization} = \Delta G^o_{Neutralization} + RT \ln \left({}^{[H_2O]}/_{[H^+][OH^-]}\right)$

$\Delta G_{Neutralization} = \Delta G^o_{Neutralization} - RT \ln [H^+] - RT \ln [OH^-]$

$\Delta G_{Neutralization} = \Delta G^o_{Neutralization} - RT\ 2.303 (\log[H^+] + \log [OH^-])$

$\Delta G_{Neutralization} = \Delta G^o_{Neutralization} - RT\ 2.303 (-pH - pOH)$

$\Delta G_{Neutralization} = \Delta G^o_{Neutralization} + RT\ 2.303 (pH + pOH)$

$\Delta G_{Neutralization} = \Delta G^o_{Neutralization} + RT\ 2.303 (pH_A + 14 - pH_B)$,

where pH_A = pH of acidic electrolyte and pH_B = pH of alkaline electrolyte

$\Delta G_{Neutralization} = \Delta G^o_{Neutralization} + RT\ 2.303 (pH_A - pH_B) + RT\ 2.303*14$

$\Delta G_{Neutralization} = \Delta G^o_{Neutralization} - RT\ 2.303\ \Delta pH + RT\ 2.303*14$ ($pH_B > pH_A$)

$\Delta G_{Neutralization} = -79.8 - 5.7\Delta pH + 79.8$

$\Delta G_{Neutralization} = -5.7\ \Delta pH$

$E = {}^{-\Delta G}/_{nF} = 0.059\ \Delta pH$ …….. **equation S4**

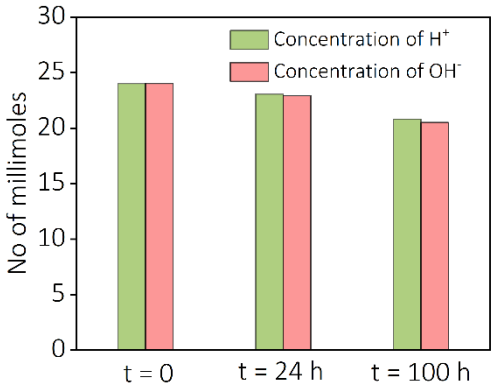

Fig. S4. H^+/OH^- dual ion concentrations before and after keeping the fuel purifier under open circuit condition for various time intervals.

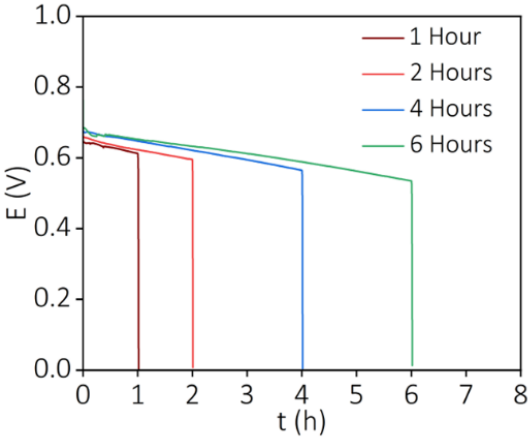

Fig. S5. Galvanostatic polarizations at 40 mA/cm^2 for different amounts of H_2 as the anodic feed gas stream.

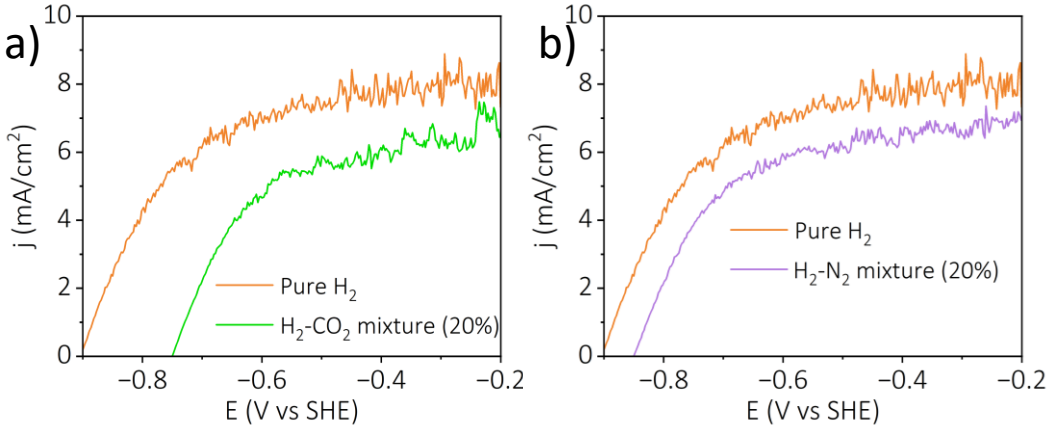

Fig. S6. Rotating disk electrode measurements during hydrogen oxidation reaction at 1600 rpm at a scan rate of 5 mV/s on a PtRu/C electrode for (a) H_2-N_2 (80:20) binary mixture and (b) H_2-CO_2 (80:20) binary mixture.

Table S1: Comparison table of limiting current densities and overpotential (at 3 mA/cm^2) for various gas mixtures on a Pt-Ru/C electrode.

Impure Mixtures	Limiting Current (mA/cm^2)	Overpotential (mV) (at 3 mA/cm^2)
Pure H_2	7.9	0
H_2-N_2 (20%)	6.9	61
H_2-CO_2 (20%)	6	157
H_2-CO (1000 ppm)	4.3	162
H_2-H_2S (1000 ppm)	7.3	6

Section S1

Half-cell chemistry of binary mixture

Linear sweep voltammogram has been recorded at a scan rate of 5 mV/s with a Pt based electrodes at a rotation of 1600 rpm for impure gas mixtures in 1 M NaOH solution. In case of H_2-N_2 mixture (20 %), a shift in the oxidation potential with a decrease in the limiting current density compared to pure H_2 is majorly attributed to the decrease in the partial pressure of hydrogen in the mixture (Fig. S6a and Table S1). However, for the H_2-CO_2 mixture (20 %), the impurity (CO_2) can chemically react with the hydroxyl ions which will eventually decrease the pH of the solution. The noticeable positive shift in the H_2 oxidation potential in H_2-CO_2 mixture compared to pure H_2 can be attributed to this chemical consumption of OH^- by CO_2 (Fig. S6b, Table S1).

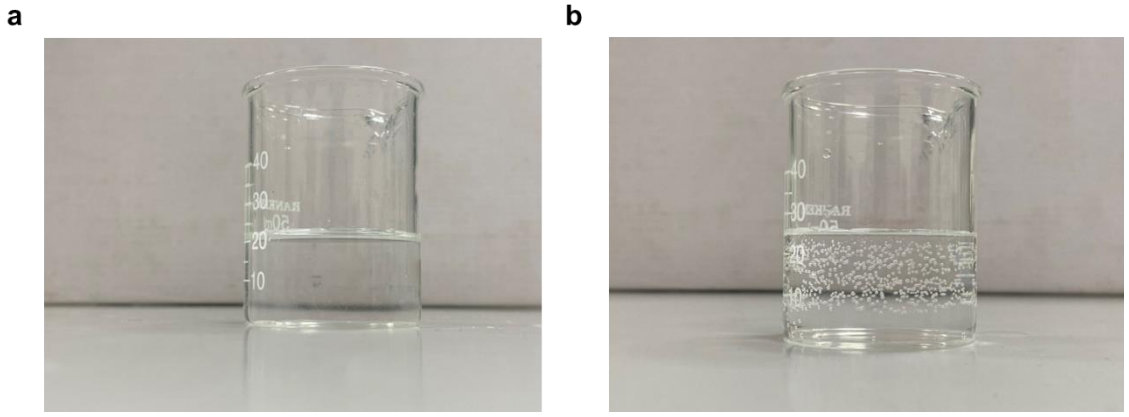

Fig. S7. Photographs of the anolyte used in H_2-CO_2 mixture separation (a) before and (b) after dilute acid (0.1 M HCl) treatment.

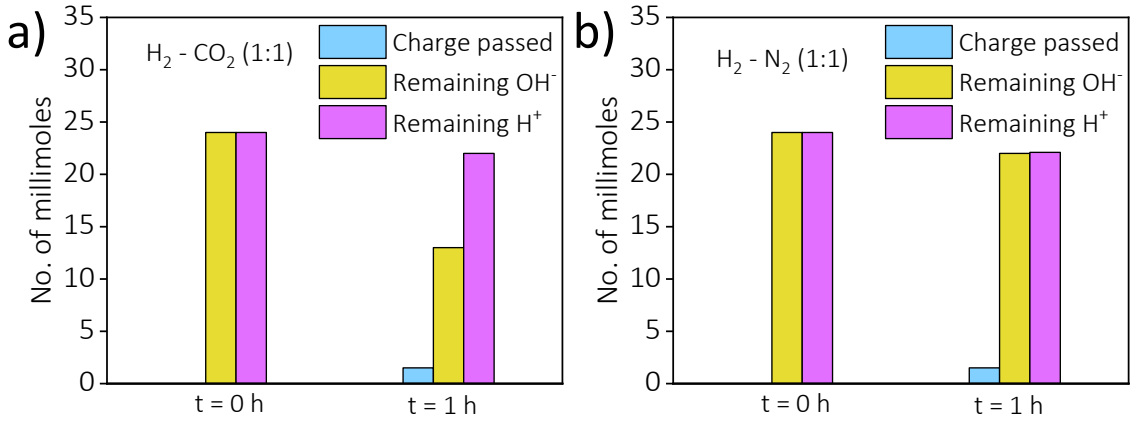

Fig. S8. Pre and post purification H^+/OH^- dual ion concentrations and the charge passed during galvanostatic polarization at 40 mA/cm^2 for 1 hour with a) H_2-CO_2 (1:1) and b) H_2-N_2 (1:1) binary mixtures.

Calculation S3

Quantification of Hydrogen

Charge passed during 40 mA constant current test for 2 hours = (2 * 3600 * 40 * 10^{-3}) C

= 288 C

Moles corresponding to the charge passed = (288/96484) = 0.002985 mol

= 2.985 mmol

To evolve one H_2 molecule there is a requirement of 2 electrons.

So, theoretically the amount of evolved H_2 = (2.985/2) = 1.4925 mmol

At room temperature (298 K) 1 mol of gas is equivalent to 24.45 L.

So, the theoretical amount of evolved H_2 gas = (24.45 * 1.4925 * 10^{-3}) = 36.49 mL

Faradaic Efficiency Calculation

1) Only H_2 gas as feed gas mixture –

Experimentally, the volume of evolved H_2 gas = 35.5 mL

Faradaic Efficiency = (35.50/36.49) * 100 = 97.29 %

2) 1:1 H_2 and N_2 mixture as feed gas –

Experimentally, the volume of evolved H_2 gas = 34.70 mL

Faradaic Efficiency = (34.70/36.49) * 100 = 95.1 %

3) 1:1 H_2 and CO_2 mixture as feed gas –

Experimentally, the volume of evolved H_2 gas = 30.5 mL

Faradaic Efficiency ＝ (30/32.78) * 100 = 93 %

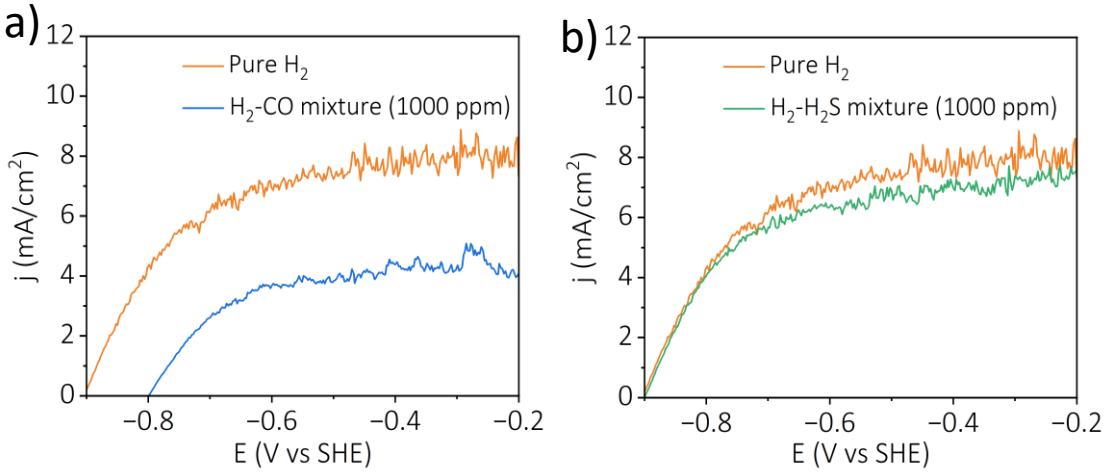

Fig. S9. Rotating disk electrode measurements during hydrogen oxidation reaction at 1600 rpm at a scan rate of 5 mV/s on a PtRu/C electrode for (a) H_2-CO binary mixture (1000 ppm CO), and (b) H_2-H_2S binary mixture (1000 ppm H_2S).

Section S2

Half-cell chemistry of binary poisonous mixture

Linear sweep voltammograms has been performed at a scan rate of 5 mV/s with Pt-Ru/C electrode at a rotation of 1600 rpm for impure gas mixtures in 1 M NaOH solution. In case of H_2-CO mixture (1000 ppm), the limiting current density is comparatively lower and the oxidation potential is positively shifted which are attributed to the adsorption of CO on to Pt domains[2,3] (Fig. S9a, Table S1), however a very stable limiting current demonstrates the capability of PtRu electrode to resist CO poisoning in a bifunctional pathway well reported in the literature[4,5]. When H_2-H_2S mixture (1000 ppm) was purged into the electrolyte, the slight decrease in limiting current density compared to pure hydrogen is observed which may be due to the slow adsorption of sulphur on to the electrode surface [6] (Fig. S9b, Table S1).

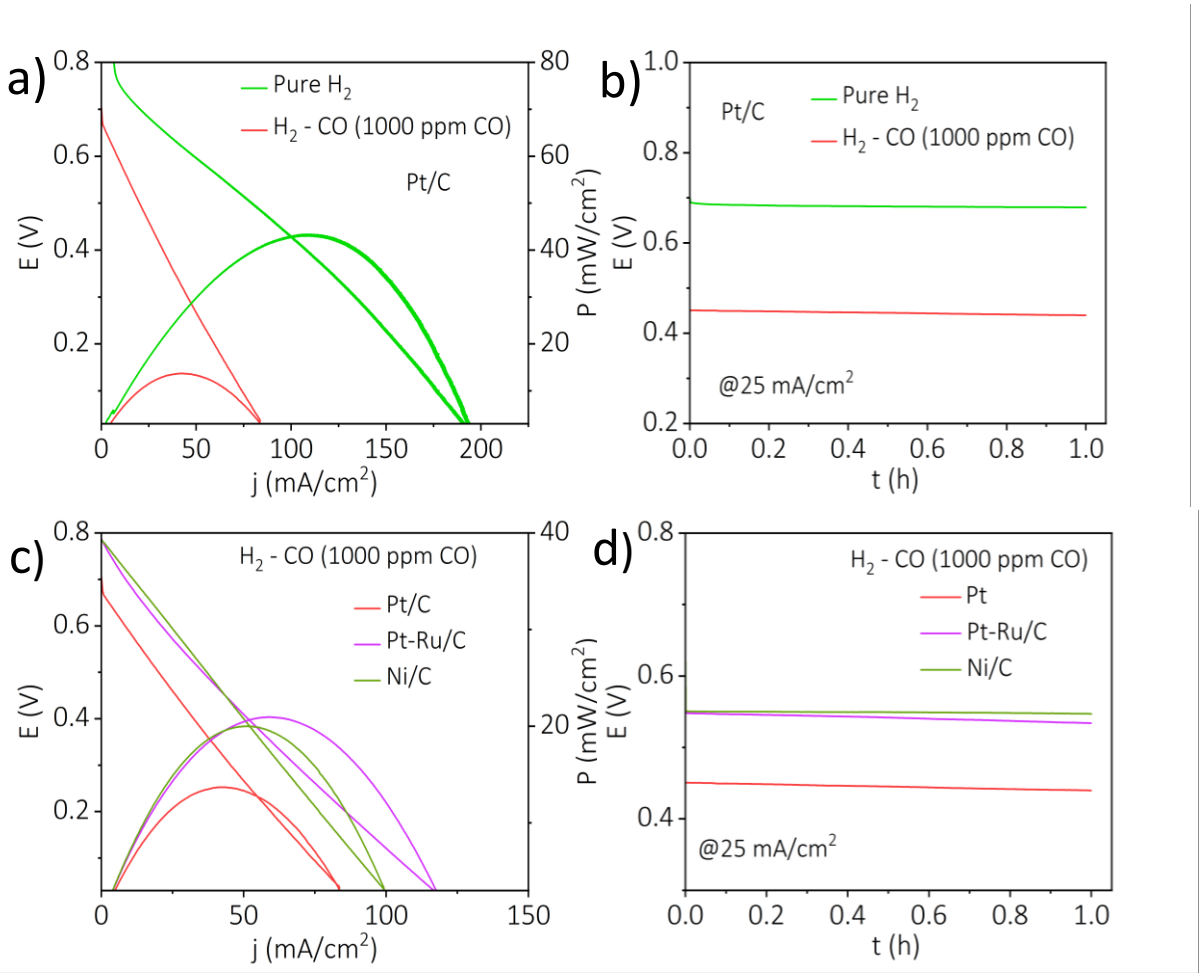

Fig. S10: a) Polarization curves and b) galvanostatic polarizations at a constant current density of 25 mA/cm^2 for the fuel purifier with pure H_2 and H_2-CO (1000 ppm CO) binary mixture as feed gas streams. c) Polarization curves and d) galvanostatic polarizations at a constant current density of 25 mA/cm^2 for the device with H_2-CO (1000 ppm CO) binary mixture as feed gas streams with Pt/C, Pt-Ru/C and Ni/C as anodic electrocatalysts.

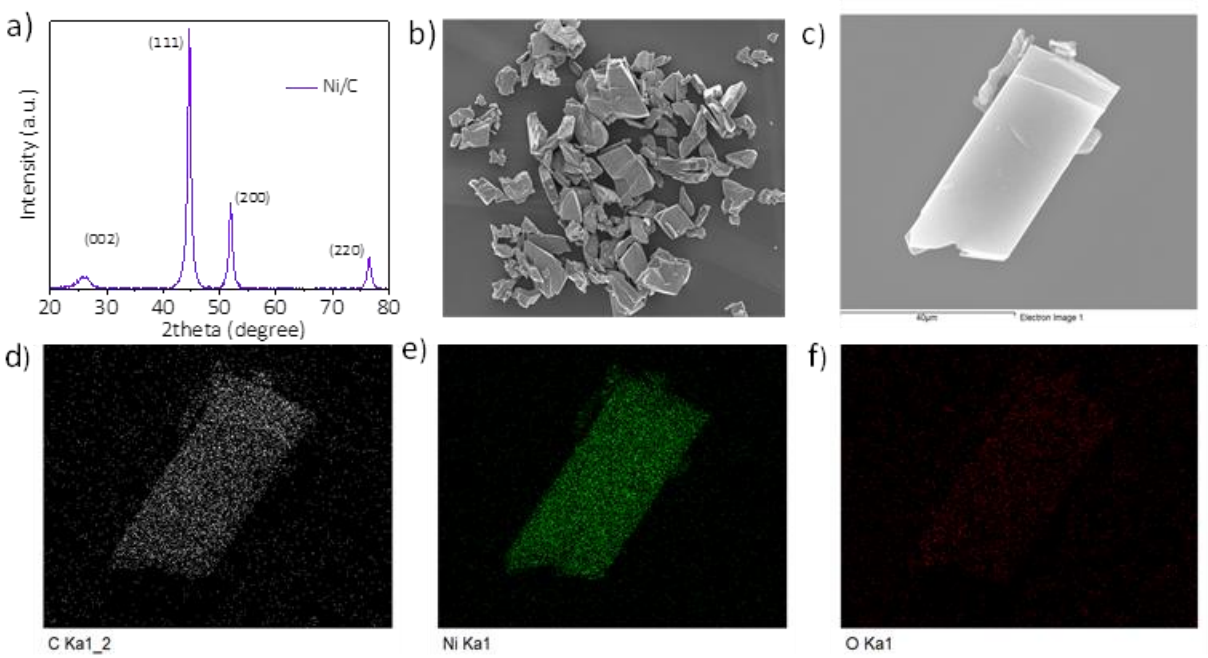

Fig. S11: a) XRD pattern b) FESEM image and (c) region of EDAX elemental mapping. Elemental mapping images for (d) carbon (e) nickel and (f) oxygen of C embedded Ni nanoparticles.

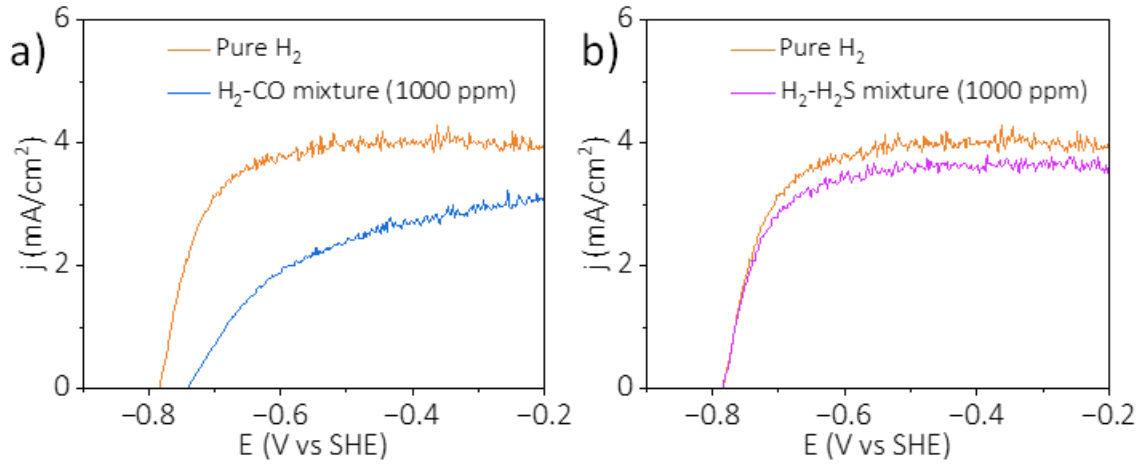

Fig. S12: Rotating disk electrode measurements during hydrogen oxidation reaction at 1600 rpm at a scan rate of 5 mV/s on a Ni based electrode for (a) H_2-CO binary mixture (1000 ppm CO), and b) H_2-H_2S binary mixture (1000 ppm H_2S) in 1 M NaOH solution.

Section S3

Half-cell chemistry of Ni/C catalyst with binary poisonous mixture

This catalyst is utilized for half-cell studies with pure H_2, H_2-CO mixture (1000 ppm CO) and H_2-H_2S mixture (1000 ppm H_2S). In case of H_2-CO mixture (1000 ppm CO), as observed in the case of Pt, the limiting current density is slightly lower with a shift in the oxidation potential to more positive values which are attributed to the adsorption of CO on to electrocatalytic domains (Fig. S11a). When H_2-H_2S mixture (1000 ppm H_2S) was purged into the electrolyte, a decrease in limiting current density compared to pure hydrogen is observed which may be due to the adsorption of sulphur on to the electrode surface, (Fig. S12b).

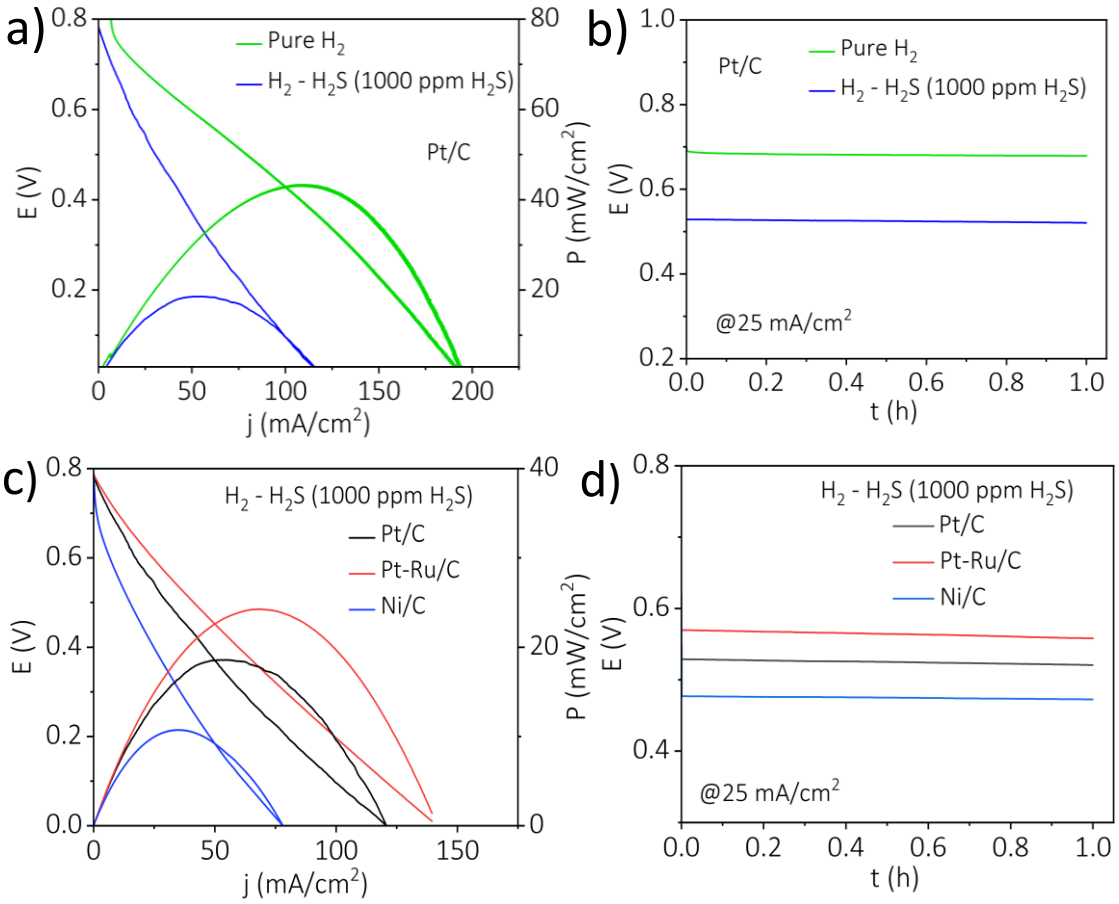

Fig. S13: a) Polarization curves (b) galvanostatic polarizations at a constant current density of 25 mA/cm^2 for the device with pure H_2 and H_2-H_2S (1000 ppm H_2S) binary mixture as feed gas streams. c) Polarization curves and d) galvanostatic polarizations at a constant current density of 25 mA/cm^2 for the device with H_2-H_2S (1000 ppm H_2S) binary mixture as feed gas streams with Pt/C, Pt-Ru/C and Ni/C as anode electrocatalysts.

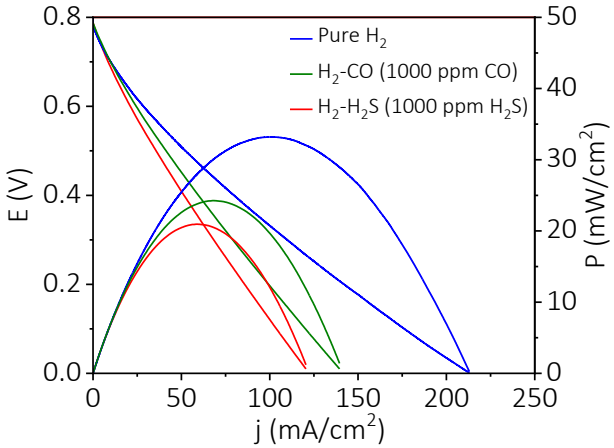

Fig. S14. Polarization curves for Pt-Ru/C based fuel purifying device with pure H_2, H_2-CO (1000 ppm CO) and H_2-H_2S (1000 ppm H_2S) binary mixtures as feed gas streams.

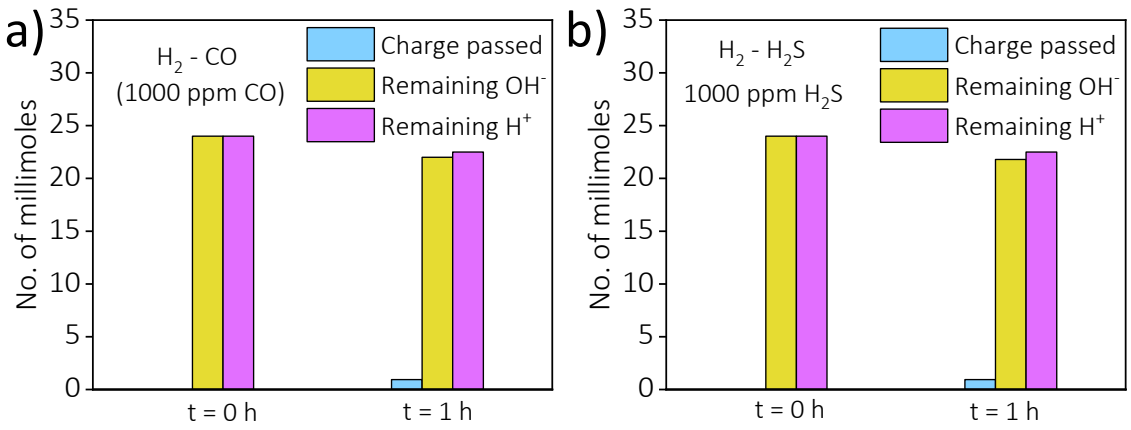

Fig. S15. Pre and post purification H^+/OH^- dual ion concentrations and the charge passed during galvanostatic polarization at 25 mA/cm^2 in 1 hour with a) H_2-CO (1000 ppm CO) binary gas mixture b) H_2-H_2S (1000 ppm H_2S) binary gas mixture as anodic feed gas streams.

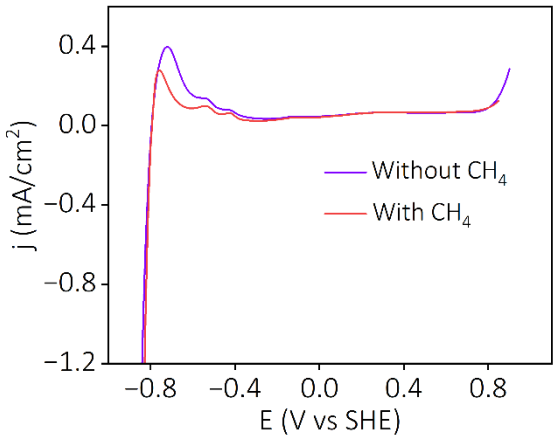

Fig. S16. Comparison of linear sweep voltammogram of Pt electrode in 1 M NaOH in the presence of H_2 and H_2 + CH_4 mixture (1:1).

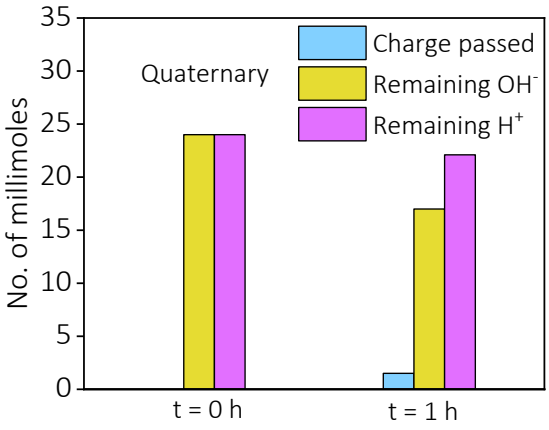

Fig. S17. Pre and post purification H^+/OH^- dual ion concentration and the charge passed during galvanostatic polarization at 40 mA/cm^2 for 1 hour with quaternary gas mixture as anodic feed gas stream.

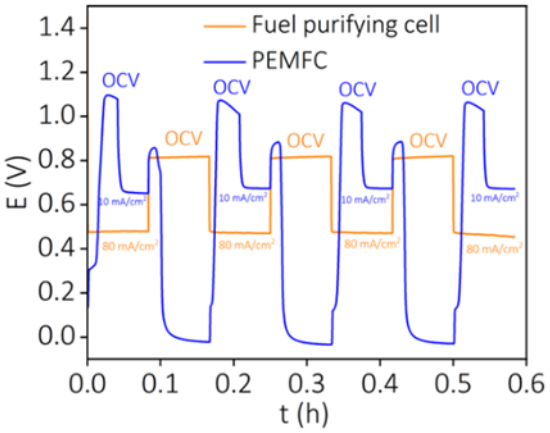

Fig. S18. Fuel purifying device directly serving as a fuel reservoir for a PEMFC in a tandem configuration.

Half-cell reactions and full cell reactions with quaternary gas mixture

Anodic Half Cell Reaction

$(H_2 + N_2 + CO_2 + CH_4) + 2OH^- \leftrightarrow 2H_2O + 2e^-$ **(equation S5)**

Cathodic Half Cell Reaction

$2H^+ + 2e^- \leftrightarrow H_2$ **(equation S6)**

Overall Cell Reaction

$(H_2 + N_2 + CO_2 + CH_4) + 2H^+ + 2OH^- \leftrightarrow 2H_2O + H_2$ **(equation S7)**

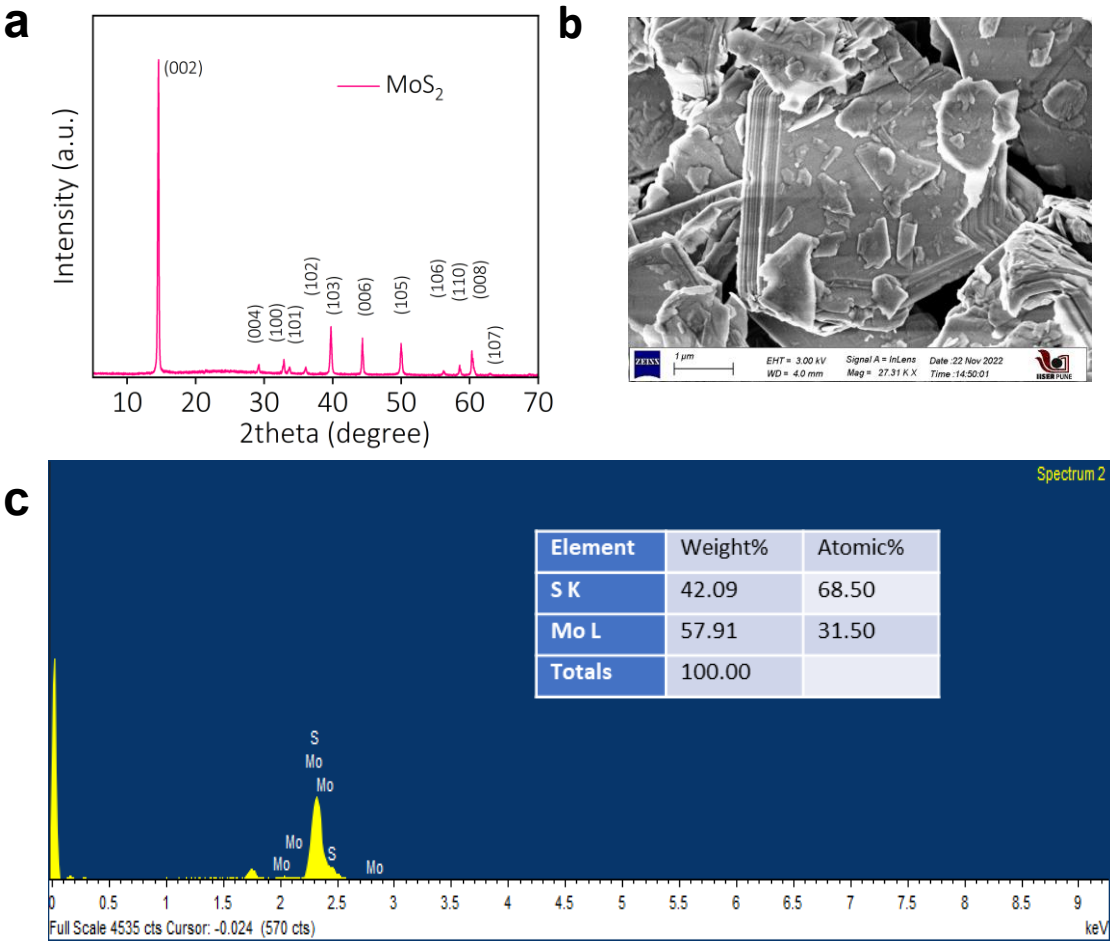

Fig. S19. (a) XRD, (b) SEM image and (c) EDX spectrum of as synthesized MoS_2.

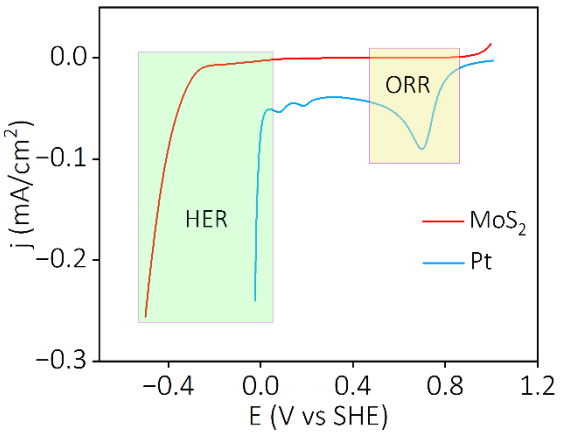

Fig. S20. Linear sweep voltammogram of Pt and MoS_2 electrode in presence of oxygen in 0.5 M H_2SO_4 at a scan rate of 20 mV/s.

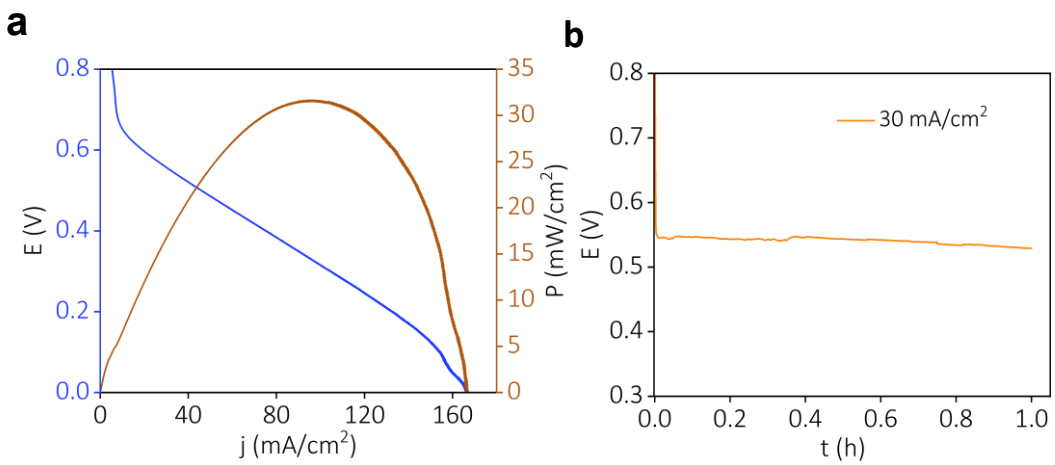

Fig. S21. (a) Polarization curve and (b) galvanostatic polarization (at 30 mA/cm^2) of the purifying device equipped with Pt/C anodic electrocatalyst and MoS_2 based cathodic electrocatalyst.

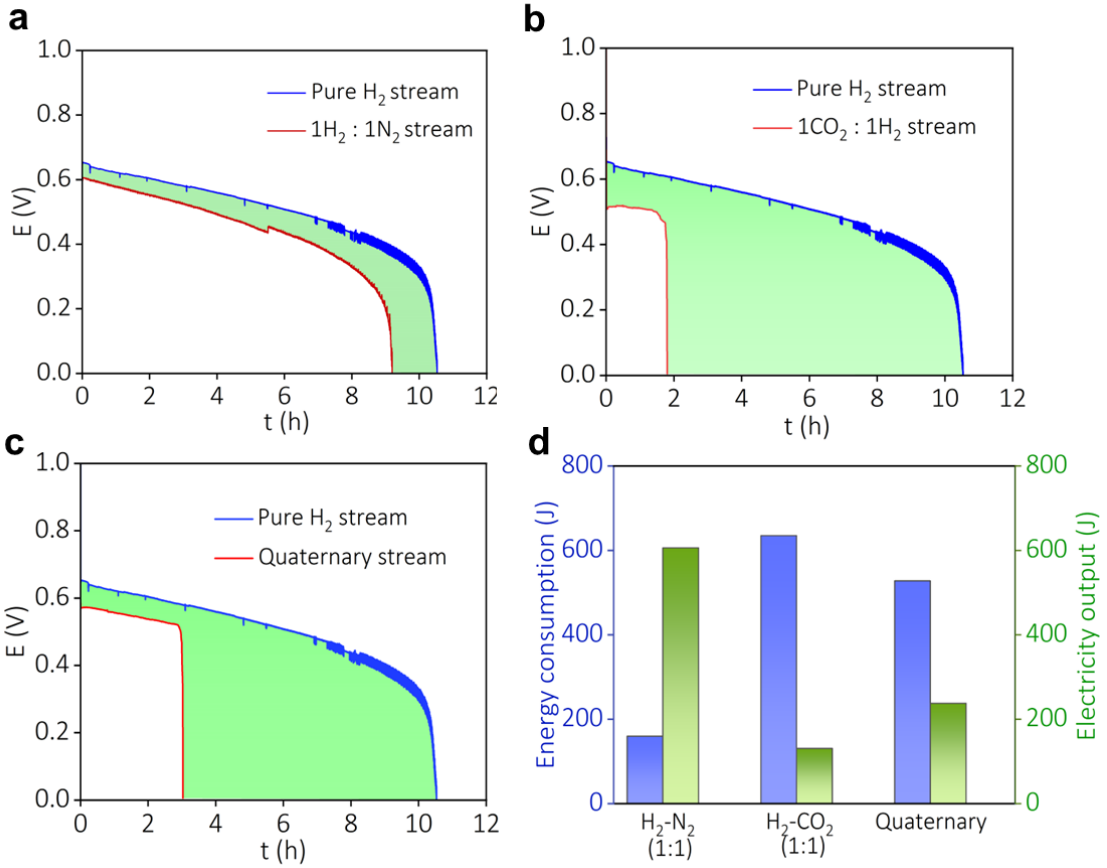

Fig. S22. Galvanostatic polarization at current density of 40 mA/cm^2 for (a) H_2-N_2 (1:1) binary mixture, (b) H_2-CO_2 (1:1) binary mixture and (c) quaternary mixture (CO_2: CH_4: N_2: H_2 = 20:1:4:75). (d) Energy consumption and electrical energy output for the gas mixtures.

Section S4

Energy Calculation

It is to be noted that in the proposed device the water formation energy is harvested as electrical driving force by utilizing H_2 redox. However, the presence of impurity lowers the extent to which this interconversion happens. Simultaneously, pure hydrogen is produced at the cathodic half-cell at the expense of this energy loss. So, the loss in the amount of electrical energy output due to the impurity can be correlated to the energy required to generate pure hydrogen on the

cathodic side. If this purified hydrogen stream from the cathodic outlet is fed to the anodic half-cell of another spontaneous fuel purifier (at the same set of conditions as in the case of impure stream), the voltage output should be similar in magnitude to that of pure hydrogen, however the time of operation should be lower. The difference should be the energy expended for fuel purification which should be similar to the loss in electrical energy due to the impurity. To further prove that the decrease in the electrical energy output is not simply due to the decrease in the concentration of hydrogen, we have calculated the energy consumption for H_2-CO_2 (1:1) mixture and the quaternary mixture, where in the impurity, (CO_2) can chemically consume the OH^-. It is found that the energy consumption during fuel purification is high for H_2-CO_2 (1:1) mixture and quaternary mixture (CO_2: CH_4: N_2: H_2 = 20: 1: 4: 75) compared to H_2-N_2 (1:1) mixture, Fig. S22. In such a case, the energy required for purification is much higher than what is predicted by the Nernst equation (by the decrease in H_2 partial pressure) and the impurity can independently affect the overall electrical energy output, (Fig. S22d). In the same way, the energy for H_2-CO_2 (1:1) and quaternary mixture are determined (Fig. S22, Calculation S4 and Calculation S5). The energy consumption for H_2-CO_2 (1:1) binary mixture and quaternary mixture is pretty high due to the chemical consumption of hydroxyl ion during the process. Nevertheless, the spontaneous fuel purifier offers an approach for simultaneous fuel purification and CO_2 capture (as carbonate) during electricity production.

Calculation S4

Energy consumption for purification

A) Case 1: $1H_2$:$1N_2$ binary mixture

From Fig. S22a

Area of the green shaded portion = Area under the curve with pure H_2 stream as anodic feed (blue trace in Fig. S22a) – Area under the curve with binary mixture of $1H_2$: $1N_2$ as anodic feed (maroon trace in Fig. S22a)

= 19155.2 – 15156.6 V. s

= 3998.6 V. s

Energy = 3998.6 * 40 * 10^{-3} A. V. s

= 159.94 A. V. s

= 159.94 W. s

= **159.94 J**

B) Case 2: $1H_2$:$1CO_2$ binary mixture

From Fig. S22b

Area of the green shaded portion = Area under the curve with pure H_2 stream as anodic feed (blue trace in Fig. S22b) – Area under the curve with binary mixture of $1H_2$: $1CO_2$ as anodic feed (maroon trace in Fig. S22b)

=19155.2 – 3256.8 V. s

=15898.4 V. s

Energy = 15898.4 * 40 * 10^{-3} A. V. s

= 635.93 W. s

= **635.93 J**

C) Case 3: Quaternary mixture

From Fig. S22C

Area of the green shaded portion = Area under the curve with pure H_2 stream as anodic feed (blue trace in Fig. S22c) – Area under the curve with quaternary mixture as anodic feed (red trace in Fig. S22c)

= 19155.2 – 5940 V. s

= 13215.2 V. s

Energy = 13215.2 * 40 * 10^{-3} A. V. s

= 528.6 W, s

= **528.6 J**

Calculation S5

Amount of pure H_2 produced during the purification of $1H_2$:$1N_2$ binary mixture = **163.5 mL**

The energy consumption for purification per 1 mole of pure H_2 = (159.94*24450)/163.5

= **23.92 kJ/mol**

Electricity energy output per 1 mole of pure H_2 = (606.264*24450)/163.5

= **90.66 kJ/mol**

Calculation S6

Electricity energy output

A) Case 1: $1H_2$:$1N_2$ binary mixture

Area under the curve with binary mixture of $1H_2$: $1N_2$ as anodic feed (maroon trace in Fig. S22a)

= 15156.6 V. s

Energy = 15156.6 * 40 * 10^{-3} A. V. s

= 606.264 W. s

= **606.264 J**

B) Case 2: $1H_2$:$1CO_2$ binary mixture

Area under the curve with binary mixture of $1H_2$: $1CO_2$ as anodic feed (maroon trace in Fig. S22b)

= 3256.8 V. s

Energy = 3256.8 * 40 * 10^{-3} A. V. s

= 130.27 W. s

= **130.27 J**

C) Case 3: Quaternary mixture

Area under the curve with quaternary mixture as anodic feed (red trace in Fig. S22c)

= 5940 V. s

Energy = 5940 * 40 * 10^{-3} A. V. s

= 237.6 W. s

= **237.6 J**

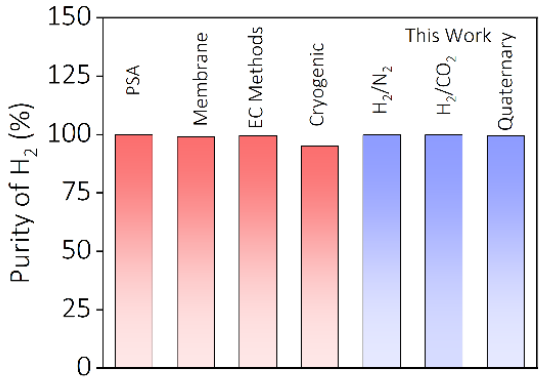

Fig. S23. Comparison of purity of hydrogen fuel obtained from the spontaneous fuel purifying device with other purification techniques. (Reference are given in the main manuscript).

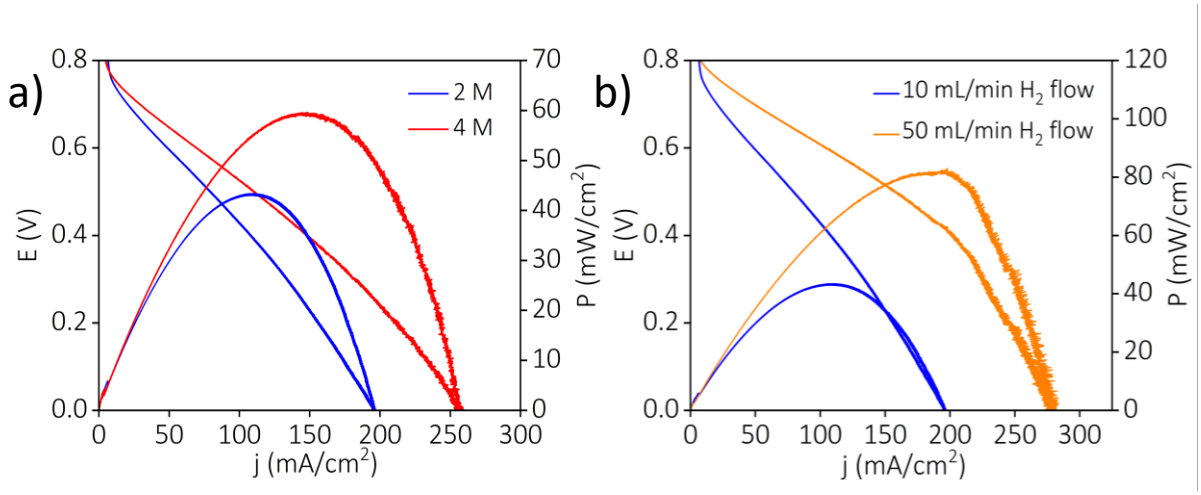

Fig. S24. a) Polarization curves of the fuel purifier with 2 M (2 M NaOH as anolyte, and 1 M H_2SO_4 as catholyte, blue trace) and 4 M (4 M NaOH as anolyte, and 2 M H_2SO_4 as catholyte, red trace) concentrations of H^+/OH^- dual ions. Anodic feed gas is H_2 at 10 mL/min. b) Polarization curves of the fuel purifier with 2 M concentrations of H^+/OH^- dual ions at 10 mL/min (blue trace) and 50 mL/min (orange trace) of H_2 flow rates.

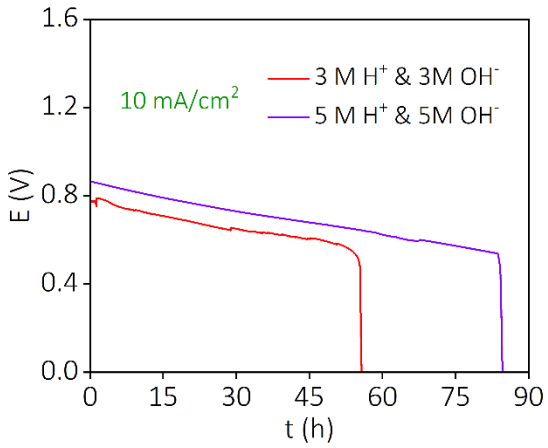

Fig. S25. Long term performance of the fuel purifier when a constant current of 10 mA/cm^2 is drawn from the device, with 3 M (red trace) and 5 M (violet trace) H^+/OH^- dual ion concentration.

Table S2: Catalyst loading used at the anodic and cathodic half-cells of the spontaneous fuel purifier.

	Cathode		Anode		
Catalyst	MoS_2/rGO (MoS_2: rGO = 1:4)	Pt on Ti mesh	Pt-Ru/C (PtRu:C=2:3) (Pt:Ru = 2:1)	Ni/C (Ni:C = 3 :2)	Pt/C (Pt:C = 2:3)
Amount	2 mg/cm^2	1.5 mg/cm^2	1 mg/cm^2	1 mg/cm^2	1 mg/cm^2

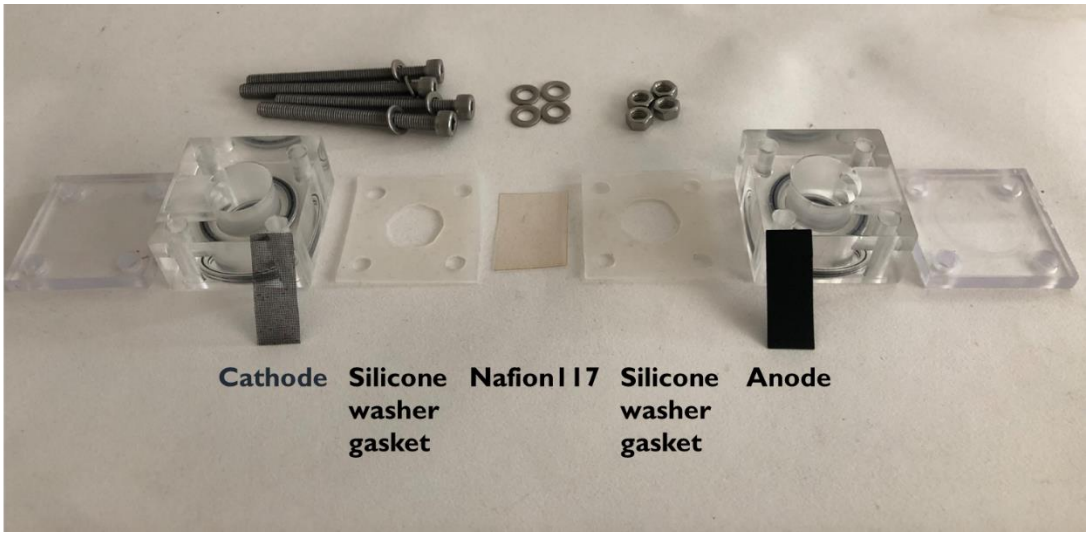

Fig. S26. Architectural components of the two-compartment cell for harvesting the water formation energy.

References

1. M. Yoo, S. J. Han and J. H. Wee, *J. Environ. Manage.*, 2013, **114**, 512–519.
2. Q. Li, R. He, J.-A. Gao, J. O. Jensen and N. J. Bjerrum, *J. Electrochem. Soc.*, 2003, **150**, A1599.
3. J. Y. Tilquin, R. Côté, D. Guay, J. P. Dodelet and G. Denès, *J. Power Sources*, 1996, **61**, 193–200.
4. T. Yajima, H. Uchida and M. Watanabe, *J. Phys. Chem. B*, 2004, **108**, 2654–2659.
5. M. J. Lee, J. S. Kang, Y. S. Kang, D. Y. Chung, H. Shin, C. Y. Ahn, S. Park, M. J. Kim, S. Kim, K. S. Lee and Y. E. Sung, *ACS Catal.*, 2016, **6**, 2398–2407.
6. W. Dong, C. Xu, W. Zhao, M. Xin, Y. Xiang, A. Zheng, M. Dou, S. Ke, J. Dong, L. Qiu and G. Xu, *ACS Appl. Energy Mater.*, 2022, **5**, 12640–12650.